AIP | Applied Physics Letters

A two-dimensional nanopatterned thin metallic transparent conductor with high transparency from the ultraviolet to the infrared

Qing Guo Du, Krishnan Sathiyamoorthy, Li Ping Zhang, Hilmi Volkan Demir, Chan Hin Kam et al.

Citation: Appl. Phys. Lett. **101**, 181112 (2012); doi: 10.1063/1.4765341
View online: http://dx.doi.org/10.1063/1.4765341
View Table of Contents: http://apl.aip.org/resource/1/APPLAB/v101/i18
Published by the American Institute of Physics.

A two-dimensional nanopatterned thin metallic transparent conductor with high transparency from the ultraviolet to the infrared

Qing Guo Du,[1,2] Krishnan Sathiyamoorthy,[1] Li Ping Zhang,[2] Hilmi Volkan Demir,[1,3] Chan Hin Kam,[1,a)] and Xiao Wei Sun[1,b)]

[1]*LUMINOUS, Center of Excellence for Semiconductor Lighting & Displays, School of Electrical and Electronic Engineering, Nanyang Technological University, Nanyang Avenue, Singapore 639798, Singapore*
[2]*Institute of High Performance Computing, 1 Fusionopolis Way, #16-16 Connexis North, Singapore 138632*
[3]*Department of Electrical and Electronics Engineering, Department of Physics, and UNAM – National Nanotechnology Research Center, Bilkent University, Ankara 06800, Turkey*

(Received 7 February 2012; accepted 18 October 2012; published online 1 November 2012)

The optical properties of a two-dimensional nanohole patterned aluminum thin film in hexagonal lattice are studied. The transmission dip can be moved out from the visible range by manipulating the lattice constant. The resulting nanopatterned thin film is demonstrated to exhibit a high transparency in a wide wavelength range. The origins of the transmission dip and the transmission drop are explained. For constant resistance, thicker films with a larger filling ratio lead to better transmittance in the visible range. Angular response of the nanopatterned metallic film is also analyzed, and transmittances using several other metals are compared. © *2012 American Institute of Physics*. [http://dx.doi.org/10.1063/1.4765341]

Transparent conductors (TCs) are essential components of modern optoelectronic devices, including solar cells, flat panel displays, and light emitting diodes (LEDs). Most of the optoelectronic devices having a TC are fabricated on indium tin oxide (ITO) coated substrates because of the relatively high transparency of ITO in the visible range and its low sheet resistance. However, ITO is costly because of the limited source of indium.[1] Moreover, ITO is brittle for devices on flexible substrates.[1] Due to these disadvantages of ITO, researchers are now seeking alternatives, which include metallic nanogratings,[2–5] metallic nanomeshes,[6,7] ultra thin metallic films,[8,9] carbon nanotube networks,[10,11] and graphenes.[12–14]

It is known that, thanks to surface plasmon polariton (SPP), the transmission enhancement of optically thick nanopatterned metal films can be realized.[15,16] However, the enhancement is only in a narrow wavelength range. This cannot be applied to optoelectronic devices that need high transparency in a wide wavelength range such as flat panel displays and solar cells. When the film thickness of nanopatterned metallic films is within a few or tens of nanometers, the optical properties become quite different from those of the optically thick metallic films. One-dimensional (1D) nanopatterned thin metallic film has been studied both theoretically and experimentally.[2–5,17] For the two-dimensional (2D) case, the studies are mainly focused on the transmission suppression in a narrow wavelength range where high optical transmission is anticipated.[18–20] There already have a few experimental papers trying to fabricate 2D nanopatterned metallic electrodes.[21,22] Unfortunately, the transmittance is not high enough in a wide wavelength range. Till now, there is no theoretical analysis on the optical properties of 2D nanopatterned metallic thin films that can be used as a potential candidate for TC over a wide spectral region. In this letter, we report that high transparency in a wide wavelength range from ultraviolet (UV) to infrared (IR) with a relatively low sheet resistance can be achieved in metal thin films with a hexagonal lattice nanohole array.

Inset of Fig. 1(a) shows the schematic of the 2D nanohole patterned metallic thin film for the study. The nanopatterned metallic thin film structure is arranged in the *x*-*y* plane with a hexagonal lattice and surrounded by air. Light is directly incident on the film along the z direction. Periodic boundary conditions are used in the *x*, *y* directions and perfectly match layer (PML) boundary condition is used in the *z* direction. The simulation region is chosen in one unit

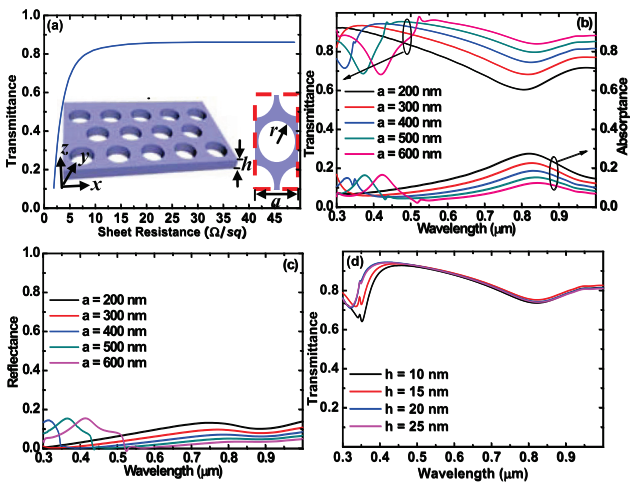

FIG. 1. (a) Average transmittance from 0.3 μm to 1.0 μm of different sheet resistance with various *f*, *a* and *h* are fixed at 400 nm and 20 nm, respectively. Inset shows the schematics of 2D nanohole patterned metallic thin film arranged in hexagonal lattice. Left side shows the 3D view and right side shows the top view of the nanopatterned structure. Simulation area of one unit cell is indicated with the red dashed line. (b) Transmittance and absorption, and (c) reflection spectra of the nanohole Al thin film for various lattice constants with $f = 0.8$ and $h = 20$ nm. (d) Transmittance spectra of the nanohole films with different thicknesses, while keeping their sheet resistance constant.

[a)]Electronic mail: echkam@ntu.edu.sg.
[b)]Author to whom correspondence should be addressed. Electronic mail: exwsun@ntu.edu.sg.

cell within one period in the x and y directions indicated by the dashed line in the inset in Fig. 1(a). The top view of the unit cell is shown in right side of inset in Fig. 1(a). The lattice constant is indicated as a, the radius of nanohole is represented by r, and the film thickness is h. The finite-difference time-domain (FDTD) method is employed for all spectra calculations using Lumerical FDTD Solutions, a commercial FDTD software package.

Before analyzing optical properties of the nanopatterned metallic thin film, the other important parameter which should be considered is the sheet resistance because a good candidate for TCs needs both high transparency and low sheet resistance. The sheet resistance of a uniform metallic thin film is given by $R_{sh} = 1/(\sigma * h) = \rho/h$, where σ and ρ are the metal conductivity and resistivity, respectively, and h is the film thickness, with a unit of Ω/sq. In the case of a 2D nanohole array structure, according to the percolation theory, the large scale effective conductivity is written as $\sigma_c = \sigma_0 (\phi_f - \phi_{crit})^t$,[23,24] where σ_c is the conductivity of the patterned structure, σ_0 is the conductivity of the conductor, ϕ_f is the volume fraction of the patterned conductor, ϕ_{crit} is the percolation threshold where the conductivity of the patterned structure is zero, and t is the critical exponent. The volume fraction of the patterned conductor ϕ_f here can be simplified as $(1-f)$ where f is the nanohole filling ratio in one period defined as $f = 2\pi r^2/\sqrt{3}a^2$ (the area ratio of void region and the whole unit cell). Here, for a 2D hexagonal hole patterned case, $\phi_{crit} = (1 - \frac{\pi}{2\sqrt{3}})$, where neighboring holes are just in contact with each other ($r = a/2$). According to Ref. 23, we chose $t = 1.1$.

Without loss of generality, we chose aluminum (Al), a cheap yet commonly used metal for the study here. The resistivity of Al is $\rho = 2.9 \times 10^{-8}(\Omega m)$. Fig. 1(a) shows the relationship of the sheet resistance with average transmittance from 0.3 μm to 1.0 μm with $a = 400$ nm and $h = 20$ nm by changing the hole filling ratio f. When the sheet resistance is small which means the hole is relatively small, it is obvious that the transmittance is low. Below 10 Ω/sq, with the increase of the sheet resistance, the transmittance increases rapidly. When the sheet resistance is larger than 10 Ω/sq, the transmittance increases only slightly. From Fig. 1(a), it is shown that when the sheet resistance of the nanohole patterned Al thin film is larger than 8.4 Ω/sq, the average transmittance is larger than 80%. For ITO, normally the sheet resistance is around 10–20 Ω/sq with transparency around 80%.[25] This indicates that the nanohole patterned Al thin film has comparable performance compared with ITO thin film. To obtain a reasonable sheet resistance, in the optical properties study below, we fixed $f = 0.8$ with $R_{sh} = 18.53$ Ω/sq which is reasonable for an electrode.

Fig. 1(b) shows the transmittance and absorptance spectra and Fig. 1(c) depicts the reflectance spectra separately for clarity, all over the spectral range from 300 nm to 1 μm for various lattice constants when the incident light is normal to the metallic thin film along the z direction. The transmittance changes with variation of the lattice constant from 600 nm to 200 nm. The highest transmittance for all different lattice constants is larger than 85% and close to unity at some specific wavelength for $a = 600$ nm. In the wavelength range shorter than 500 nm, there is a transmission dip. When the lattice constant is larger (for example, $a = 600$ nm), the dip is in the visible range in which we are most interested, and the transmission in the long wavelength range is relatively higher than in the other ranges. When the lattice constant decreases, the dip is blue-shifted, and the transmission in the long wavelength range only decreases slightly.

By manipulating the lattice constant, we can move the dip out of visible range, although the transmission in the long wavelength range also drops. Two reasons are attributed to the transmission dips at short wavelengths. One is the enhanced reflectance around the dip, which can be verified by the reflectance in Fig. 1(c). The reflectance at the transmission dip is larger than that of other wavelengths. The other one is the absorptance enhancement at the same wavelength as shown in Fig. 1(b). Additionally, for all the films of different lattice constants, there is a continuous transmittance drop after the maximum transmittance and reaches the next lower level at around 830 nm. This is due to interband transition absorption of Al.[6] Furthermore, this absorption peak is found to be slightly blue-shifted when the lattice constant is decreased. The wide high transparency wavelength range makes the 2D nanohole patterned metallic thin film arranged in hexagonal lattice more suitable for TC applications.

From the sheet resistance perspective, the influence of the hole radius and film thickness on transmittance is analyzed with the sheet resistance kept constant. Obviously, when the film thickness is reduced, the nanohole radius needs to be reduced to maintain a constant resistance. To study the effects of h and f on the transmittance, the spectral relationship of transmittance for 4 different thicknesses ($h = 10$ nm, 15 nm, 20 nm, 25 nm) of the thin films is plotted in Fig. 1(d) with the sheet resistance kept unchanged. Here, the lattice constant is fixed at $a = 400$ nm. The transmittance is the lowest for $h = 10$ nm, here small h and small f do not lead to better transparency. The transmittance is only slightly different for large h and large f when the optical wavelength is longer than 450 nm. For the wavelength shorter than 450 nm, the transmittance first increases with the increasing h (up to 20 nm), and then decreases slightly (up to $h = 25$ nm). The maximum amplitude transmission in this range is achieved when the thickness of the metal film approaches SPP skin depth, which is given by

$$\delta = \frac{1}{\mathrm{Im}(k_z)} = \frac{c}{\omega}\frac{1}{\mathrm{Im}(\sqrt{\varepsilon_m})}, \quad (1)$$

where k_z and ε_m are the imaginary refractive index and dielectric constant of the metal, respectively, and c is the velocity and ω is the frequency of the light.[26] For example, the calculated SPP skin depth at the surface plasmon resonance frequency of 856.55 THz (350 nm) is 23 nm. The imaginary value of the complex refractive index of Al at 856.55 THz is 4.274. As the thickness of the Al layer is close to the skin depth, SPP modes that are excited on both air-metal sides of the Al film are coupled via evanescent waves and form coupled SPP modes, which boost the total transmission significantly. Besides, an increased absorption peak at 350 nm is observed due to the interaction of the front and back SPP waves within the metal medium during SPP propagation. The 25 nm thick Al film shows slight a decrease in the transmission

as the coupling between SPP modes that are excited on the either side of the Al film is not as strong as that for 20 nm thick Al case, due to the fact that its film thickness is greater than the skin depth.

Filling the air holes with some commonly used dielectrics and organics (e.g., silicon oxide (SiO_2), silicon nitride (Si_3N_4), and Poly(3,4-ethylenedioxythiophene) poly(styrenesulfonate) (PEDOT:PSS)) is studied. Fig. 2(a) shows the transmittances of filled Al electrode. The transmittance of a thin film with 20 nm thickness is also presented as a reference. All the filled nanostructures have the same lattice constant, filling ratios, and thicknesses as the optimized unfilled metal nanostructures. For nanostructure filled with SiO_2, the transmittance is higher than that of the air hole filled nanostructure in long wavelength range from 500 nm, but in the short wavelength range, the transmittance is lower. For nanostructure filled with Si_3N_4 with refractive index larger than SiO_2, there is a significant drop in the short wavelength range. The transmittance of PEDOT:PSS is similar to that of the nanostructure filled with SiO_2. The transmittance of the Al thin film is extremely low and most of the light has been reflected. The substrate effect on the transmittance is also studied (Fig. 2(b)). When a SiO_2 substrate (glass) is used, the transmittance in short wavelength range is further dropped, but the transmittance in the long wavelength range is little influenced and remains high. The influence on the transmittance for hole-filling (with SiO_2) of the Al nanoelectrode on glass is not significant, which is similar to the substrate-free case in Fig. 2(a).

The angular dependence of the transmittance of the nanopatterned Al thin film for both transverse-electric (TE) and transverse-magnetic (TM) polarizations is studied. Here, the TM polarization is as the case when the magnetic field is in the x direction and TE polarization is defined as the case when the magnetic field is in the y direction. The structure parameters are fixed at $a = 400$ nm, $f = 0.8$, and $h = 20$ nm. Detailed relationship between transmittance spectrum and incident angle is shown in Fig. 3. For clearance, only the transmittance of 10°, 30°, and 60° of incident angle is plotted. For TE polarization as shown in Fig. 3(a), with the increase of the incident angle, the transmittance decreases in short wavelength range and increases in long wavelength range. For TM polarization as shown in Fig. 3(b), the transmittance drops in the whole wavelength range when the incident angle increases. The drop is more significant in the long wavelength

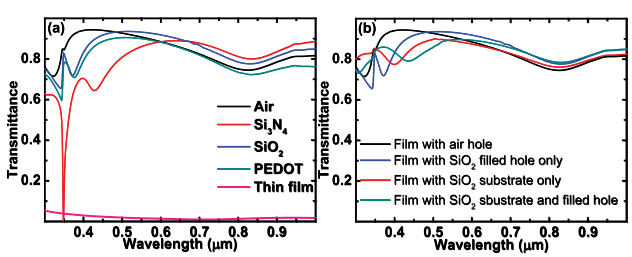

FIG. 2. (a) Transmittances of the nanohole Al thin film for various filling materials (SiO_2, Si_3N_4, and PEDOT:PSS) and a Al thin film with the same thickness. (b)Transmittances of the nanohole Al thin film with air hole, with SiO_2 filled holes only, with SiO_2 substrate only, and with both SiO_2 filled holes and substrate. Structure parameters are fixed at $a = 400$ nm, $f = 0.8$, and $h = 20$ nm.

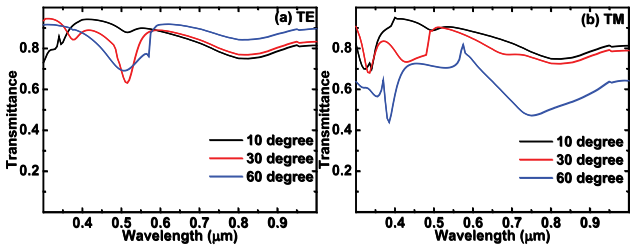

FIG. 3. Transmission spectra for (a) TE and (b) TM polarizations with incident angle of 10°, 30°, and 60°. The structure parameters are fixed at $a = 400$ nm, $f = 0.8$, and $h = 20$ nm.

range. Fig. 4(a) shows the average transmittance spectra from 300 nm to 1.0 μm of TM and TE polarization, respectively. For TE polarization, the average transmittance remains high even when the incident angle is increased to 60°, while the average transmittance of TM polarization drops to 60%.

For some applications, we may need to vary the work-function of the TC. As such, we studied the transmittance of 2D hexagonal lattice nanohole arrays made of different metals (aluminum (Al), silver (Ag), gold (Au), and nickel (Ni)), as shown in Fig. 4(b). For different metals, the optimized parameters are the same, i.e., $a = 400$ nm, $f = 0.8$, and $h = 20$ nm. Detailed spectra optimizations for different metals are not shown here. For Ag and Au nanopatterned thin films, the transmission dip cannot be moved out from the visible range because the dip tends to have a red shift when the lattice constant is reduced.[17] However, the transmittance in the long wavelength range is much better than that of other metals. The Ni film has a flatter transmission spectrum for the wavelength range from 300 nm to 1.0 μm but the average transmittance is relatively low. Al nanostructure has the best transmittance in the visible range among the four.

One of the immediate tools of fabricating the aluminum nanostructure is the electron beam lithography (EBL).[27] The drawback is that it is costly and not efficient to fabricate large area metallic transparent electrode. Another method is the polymer sphere (PS) lithography which is much cheaper than EBL.[22] But PS assembly is a bottom-up process, there may be defects generated. The third method is the anodization, again it is a self-assembly method, which is prone to generated defects.[28] The generated defects may have effect on the transmittance.[24] The influence of defects on conductivity is negligible. As the optimized dimension of the metal structure is more than 20 nm, electron mean free path is 14 nm for aluminum at room temperature, hence scattering can be ignored.[29]

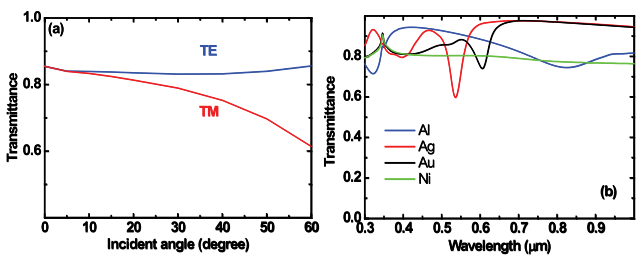

FIG. 4. (a) Average transmittance for TE and TM polarizations VS. the incident angle of the structure as in Fig. 3. (b) Transmission spectra of the structures made of metal materials Al, Ag, Au and Ni. The structure parameters are chosen as $a = 400$ nm, $f = 0.8$ and $h = 20$ nm for all metal materials here.

In conclusion, the 2D patterned Al thin film with a hexagonal lattice enables a high transparency for a wide wavelength range from UV to IR. By manipulating the lattice constant a, the transmission dip can be moved out from the visible range. The transmission dip results from the enhancement of reflectance and absorptance. The continuous transmittance drop following the maximum transmittance stems from the increasing evanescence of the light. When the sheet resistance is kept constant, larger h and larger f lead to a higher transmittance level over the wide spectral region. TE polarization allows for a better angular transmittance than TM polarization. Compared to other nanopatterned metallic films, nanopatterned Al thin film yields the best transmission spectrum in the visible wavelength range.

This work was supported by Agency for Science, Technology and Research (A*STAR) of Singapore under Grant Nos. 0921510088 and 0921010057, and Singapore National Research Foundation under Grant Nos. NRF-RF-2009-09 and NRF-CRP-6-2010-2.

[1]Z. Chen, B. Cotterell, W. Wang, E. Guenther, and S. J. Chua, Thin Solid Films **394**, 201–205 (2001).
[2]M. G. Kang and L. J. Guo, Adv. Mater. **19**, 1391–1396 (2007).
[3]M. G. Kang, M. S. Kim, J. S. Kim, and L. J. Guo, Adv. Mater. **20**, 4408–4413 (2008).
[4]M. G. Kang, T. Xu, H. J. Park, X. G. Luo, and L. J. Guo, Adv. Mater. **22**, 4378–4383 (2010).
[5]P. Kuang, J.-M. Park, W. Leung, R. C. Mahadevapuram, K. S. Nalwa, T.-G. Kim, S. Chaudhary, K.-M. Ho, and K. Constant, Adv. Mater. **23**, 2469–2473 (2011).
[6]J.-Y. Lee, S. T. Connor, Y. Cui, and P. Peumans, Nano Lett. **8**, 689–692 (2008).
[7]H. Wu, L. Hu, M. W. Rowell, D. Kong, J. J. Cha, J. R. McDonough, J. Zhu, Y. Yang, M. D. McGehee, and Y. Cui, Nano Lett. **10**, 4242–4248 (2010).
[8]B. O'Connor, C. Haughn, K. H. An, K. P. Pipe, and M. Shtein, Appl. Phys. Lett. **93**, 223304 (2008).
[9]D. S. Ghosh, L. Martinez, S. Giurgola, P. Vergani, and V. Pruneri, Opt. Lett. **34**, 325–327 (2009).
[10]Z. C. Wu, Z. H. Chen, X. Du, J. M. Logan, J. Sippel, M. Nikolou, K. Kamaras, J. R. Reynolds, D. B. Tanner, A. F. Hebard, and A. G. Rinzler, Science **305**, 1273–1276 (2004).
[11]M. Zhang, S. L. Fang, A. A. Zakhidov, S. B. Lee, A. E. Aliev, C. D. Williams, K. R. Atkinson, and R. H. Baughman, Science **309**, 1215–1219 (2005).
[12]J. B. Wu, H. A. Becerril, Z. N. Bao, Z. F. Liu, Y. S. Chen, and P. Peumans, Appl. Phys. Lett. **92**, 263302 (2008).
[13]J. B. Wu, M. Agrawal, H. A. Becerril, Z. N. Bao, Z. F. Liu, Y. S. Chen, and P. Peumans, ACS Nano **4**, 43–48 (2010).
[14]M. Cox, A. Gorodetsky, B. Kim, K. S. Kim, Z. Jia, P. Kim, C. Nuckolls, and I. Kymissis, Appl. Phys. Lett. **98**, 123303 (2011).
[15]T. W. Ebbesen, H. J. Lezec, H. F. Ghaemi, T. Thio, and P. A. Wolff, Nature **391**, 667–669 (1998).
[16]P. B. Catrysse, W. J. Suh, S. H. Fan, and M. Peeters, Opt. Lett. **29**, 974–976 (2004).
[17]P. B. Catrysse and S. Fan, Nano Lett. **10**, 2944–2949 (2010).
[18]J. Braun, B. Gompf, G. Kobiela, and M. Dressel, Phys. Rev. Lett. **103**, 203901 (2009).
[19]S. S. Xiao and N. A. Mortensen, Opt. Lett. **36**, 37–39 (2011).
[20]S. S. Xiao, J. J. Zhang, L. A. Peng, C. Jeppesen, R. Malureanu, A. Kristensen, and N. A. Mortensen, Appl. Phys. Lett. **97**, 071116 (2010).
[21]M. Green and F. T. Yi, Thin Solid Films **467**, 308–312 (2004).
[22]T. Nakanishi, E. Tsutsumi, K. Masunaga, A. Fujimoto, and K. Asakawa, Appl. Phys. Express **4**, 025201 (2011).
[23]M. Weber and M. R. Kamal, Polym. Compos. **18**, 711–725 (1997).
[24]T. H. Reilly, R. C. Tenent, T. M. Barnes, K. L. Rowlen, and J. van de Lagemaat, ACS Nano **4**, 615–624 (2010).
[25]H. S. Kwok, X. W. Sun, and D. H. Kim, Thin Solid Films **335**, 299–302 (1998).
[26]Y. H. Ye and J. Y. Zhang, Opt. Lett. **30**, 1521–1523 (2005).
[27]J. van de Groep, P. Spinelli, and A. Polman, Nano Lett. **12**, 3138–3144 (2012).
[28]P. G. Miney, P. E. Colavita, M. V. Schiza, R. J. Priore, F. G. Haibach, and M. L. Myrick, Electrochem. Solid-State Lett. **6**, B42–B45 (2003).
[29]S. Kasap, *Principles of Electronic Materials and Devices* (McGraw-Hill Higher Education, 2005).